JOURNAL OF NANO- AND ELECTRONIC PHYSICS
Vol. **7** No 3, 03003(5pp) (2015)

ЖУРНАЛ НАНО- ТА ЕЛЕКТРОННОЇ ФІЗИКИ
Том **7** № 3, 03003(5cc) (2015)

Optical Properties of Co-doped Zinc Oxide Nanoparticles, Prepared by Pulsed Laser Ablation in Liquids

A.I. Savchuk[1], I.D. Stolyarchuk[*1,2], B. Cieniek[3], A. Dzedisc[3], I.V. Hadzaman[2], I.S. Virt[2]

[1] *Department of Physics of Semiconductors and Nanostructures, Chernivtsi National University, 2, Kotsyubynsky Str., 58012 Chernivtsi, Ukraine*
[2] *Ivan Franko Drohobych State Pedagogical University, 24, I. Franko Str., 82100 Drohobych, Ukraine*
[3] *Centre for Innovation and Transfer of Natural Sciences and Engineering Knowledge, University of Rzeszow, 1, Pigonia Str., 35959 Rzeszow, Poland*

(Received 28 April 2015; published online 20 October 2015)

Results of study of $Zn_{1-x}Co_xO$ nanoparticles, which were grown by pulsed laser ablation in liquid medium (PLAL), have been presented. $Zn_{1-x}Co_xO$ nanoparticles were produced by laser ablation of ceramic plates as targets in deionized water. The structural analysis using X-ray diffraction (XRD) of nanocrystals reveals the formation of predominant (002) reflection corresponding to the hexagonal wurtzite structure without any secondary phase. The performed scanning electron microscopy (SEM) analysis suggests of the well-defined flower-like nanoparticles. In optical absorption spectra of the colloidal nanoparticles short wavelength shift of the absorption edge due to confinement effect has been observed. With increasing of cobalt content the optical absorption spectra shown a red shift of the band edge which are caused by to the *s*, *p-d* exchange interactions between the band electrons and the localized spins of magnetic impurities. In the room temperature photoluminescence spectra of $Zn_{1-x}Co_xO$ nanoparticles four main peaks were revealed, which are attributed to the band - edge transitions and vacancies or defects

Keywords: $Zn_{1-x}Co_xO$, Nanoparticles, Nanocrystal, Pulsed laser ablation in liquids, X-ray diffraction, Optical absorption, Photoluminescence.

PACS numbers: 78.67.Bf, 78.40.Fy, 78.55.Et, 79.20.Eb, 71.55.Gs, 71.70.Gm, 81.16Mk

1. INTRODUCTION

Semiconductor nanoparticles (NPs) doped with transition metal (TM) ions represent an exciting class of materials, known as diluted magnetic semiconductors (DMSs). Their key feature is the *s*, *p-d* exchange interaction between delocalized charge carriers and the magnetic dopants, which is responsible for unique physical properties of this class of materials. The DMS NPs exhibit interesting optical, magnetic and magneto-optical properties such as large Faraday rotation, giant Zeeman splitting, etc. with many potential practical applications in the field of spintronics [1, 2]. Recently the family of DMSs was increased by addition of the semiconducting oxides [3, 4].

Zinc oxide (ZnO), an optically transparent II-VI semiconductor with hexagonal wurtzite structure of C^4_{6v} ($P6_3mc$) space group, wide direct band gap (E_g ~ 3.37 eV), excitons binding energy (~ 60 meV) has been identified as a promising host material after theoretical prediction of ferromagnetism above room temperature in Mn-doped ZnO [6]. Among transition metals, cobalt is an important dopant and has been intensively investigated. However, there are suggestions that defects or vacancies may induce room temperature ferromagnetism in TM doped ZnO [5, 6]. It was shown in numerous experiments that exhibition of different magnetic behaviors depends on the fabrication conditions and sample processing.

Several methods are available for the synthesis of ZnO – based DMS nanostructures, such as a chemical vapor deposition [7] hydrothermal process [8], sol-gel method [9], co-precipitation method [10], pulsed laser deposition, etc.

In particular, pulsed laser ablation in vacuum or in gas atmosphere, has been already applied in our previous papers [11-13] to prepare ZnO : TM thin films. On the other hand, pulsed laser ablation in liquids (PLAL) is comparatively new technique for the synthesis of nanosized semiconductor materials [14-20]. PLAL technique has many advantages compared to the other growth routes such as a large number of available ablation parameters for controlling the size and shape of nanoparticles and ability of producing nanomaterials with its surface free from chemical contamination. To our knowledge, application of PLAL to fabricate undoped ZnO nanoparticles was reported in papers [15-19], but similar data on doped ZnO:TM nanoparticles are negligible [21].

Herein, we report on optical absorption and photoluminescence studies of $Zn_{1-x}Co_xO$ nanoparticles synthesized by PLAL.

2. EXPERIMENTAL SECTION

$Zn_{1-x}Co_xO$ nanoparticles were produced by laser ablation of a ceramic target in deionized water (with a resistivity of 15 MΩ cm at 20 °C). The target was irradiated using a frequency – quadrupled *Q*- switched Nd: YAG pulse laser (Continuum, Powerlite-8010). This laser was capable of producing 100 mJ of 266 nm light per pulse, laser fluence about 1.5 J/cm^2, operating at 10 Hz with pulse width of 7 ns. However, $Zn_{1-x}Co_xO$ ($0 < x \leq 0.06$) ceramic plates as targets were applied in

* istolyarchuk@ukr.net

this case. The ceramic plates were prepared as follows. Substitutional Zn-Mn-O solid solutions of different compositions were synthesized by a solid-state fusion method based on solid-state mixing of the corresponding oxides or by using of carbonates as precursors. Commercially available ZnO and $CoCO_3$ (analytical grade) were used as starting materials without any additional purification. The stoichiometric mixtures were obtained by ball milling in ethanol and drying at 100 °C for 1 h, followed by annealing in air at 700 °C for 4 h, then ball milling in ethanol again for re-homogenization and, finally, air-drying at 100 °C for 1 h. As a result, particle size of 20-50 nm was achieved. Due to electrostatic forces the synthesized powder agglomerated into cluster particles with an average size of 0.4-0.8 μm. The powder was then pressed into discs 15 mm in diameter by applying the pressure of 100 MPa.

However, for the synthesis of nanoparticles, a target was fixed at the bottom of a glass vessel on Al foil and covered by the deionized water (about 10 ml). The laser beam was steered vertically by dichroic mirror and focused by a quartz lens with focal length of 250 mm in order to get sufficient laser intensity for ablation. The reaction vessel was continuously rotated to avoid crater formation and to expose the new surface of target. The ablation process duration was typically about 40 min. Technological experiments were carried out at room temperature and atmospheric pressure. Experimental setup for deposition of thin films has been in part reported earlier [22]. After laser ablation the colloidal aqueous solution with the produced nanoparticles or the dropped layer onto Al substrate were the samples under investigations. Additionally, polyvinylalcohol (PVA) was used as a stabilizer of colloidal solution.

2.1 Experimental Set Up

The crystallographic studies were performed using X-ray Diffractometer (D8 ADVANCE X-ray Diffractometer with DAVINCI) using Cu-K_α wavelength ($\lambda = 1.54059$ Å) and scanning in 2Θ range from 10° to 70°.

The morphology of the samples was examined using Quanta 3D Dual Beam SEM/FIB scanning electron microscopy (SEM). Energy-dispersive X-ray analysis was performed using an inbuilt EDS. Optical transmission and absorption spectra between 300 and 700 nm were measured using a grating monochromator, a photodetector system and registered computer system. This setup has also served to register photoluminescence (PL) spectra. For such kind of measurements the samples were excited using a 325 nm He-Cd laser with an excitation intensity value of 10 mW).

3. RESULTS AND DISCUSSION

The X-ray diffraction (XRD) patterns of $Zn_{1-x}Co_xO$ nanoparticles are shown in Fig. 1. All intense peaks positions correspond to the standard diffraction pattern of ZnO hexagonal wurtzite with a (002) preferred orientation. With an increase in Co content ($x > 0.02$) additional diffraction peaks were observed, corresponding to (100), (101), and (102) of ZnO. No peaks corresponding to cobalt metal clusters or cobalt oxides are observed on the patterns which indicates that Co has entered the ZnO lattice without changing the wurtzite structures and systematically substituted the Zn^{2+} ions in the lattice.

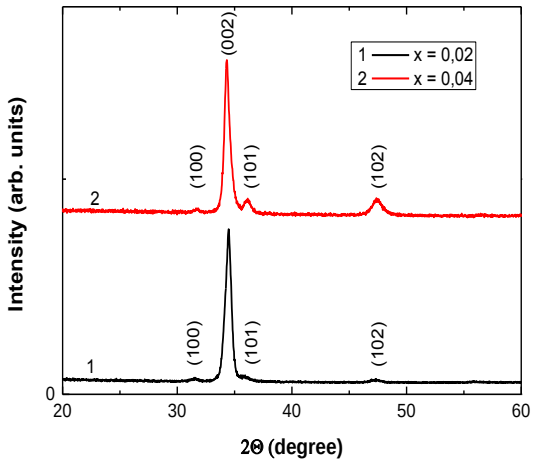

Fig. 1 – X-ray diffraction spectra of Co doped ZnO nanoparticles with various doping level

The relative intensity of the (002) peak of the $Zn_{1-x}Co_xO$ ($0 < x \le 0.06$) nanostructures exhibits stronger than other peaks, indicating that the C-axis preferred texture growth of the Co-doped ZnO nanocrystals.

Figure 2 (a, b) shows the morphology and chemical composition of obtained NPs investigated by SEM and EDS analyses. The $Zn_{1-x}Co_xO$ nanostructure (Fig. 2a) shows a flower-like morphology and small nanoparticles are filled in the inner and intermediate spaces of the nanoflowers. The observed flower-like structures consist of nanosheets with thickness about 20 nm and diameter about 50-90 nm. About similar flower-like ZnO nanostructures synthesized by chemical methods several research groups have reported recently [23-25]. The energy dispersive spectroscopy (EDS) analysis simultaneously was carried out in order to estimate the average concentration of elements. As shown in Fig. 2b carbon, zinc, aluminium, iron, cobalt and oxygen were detected. Obviously, the most intense peak is attributed to Al substrate foil as the presence of iron. The Zn, Co and O are from the formed $Zn_{1-x}Co_xO$ particle layer. In addition, C contamination was also detected. The EDS results show that the amount of zinc oxide increased when number of laser pulses is increased and the amount of Co impurity is less than in the used $Zn_{1-x}Co_xO$ targets.

UV-Vis optical measurements were carried out at room temperature. Fig. 3 shows the optical transmission spectra of colloidal $Zn_{1-x}Co_xO$ nanoparticles dispersed in polyvinylalcohol (PVA) solution. It was found that the absorption edge is blue- shifted as compared to the bulk crystal or thin films

$Zn_{0.98}Co_{0.02}O$ (with thickness of 1.2 μm) due to confinement effect. The optical transmittance spectra showed a shift in the band edge towards lower energy side with the increase of Co content. Additional absorption below the absorption edge can be seen for the $Zn_{1-x}Co_xO$ nanoparticles (Fig. 4). In particular, for Co content of $x = 0.04$ two absorption bands at about 565 nm and 654 nm have been revealed which are in agreement with already reported absorption peaks [26, 27]. This

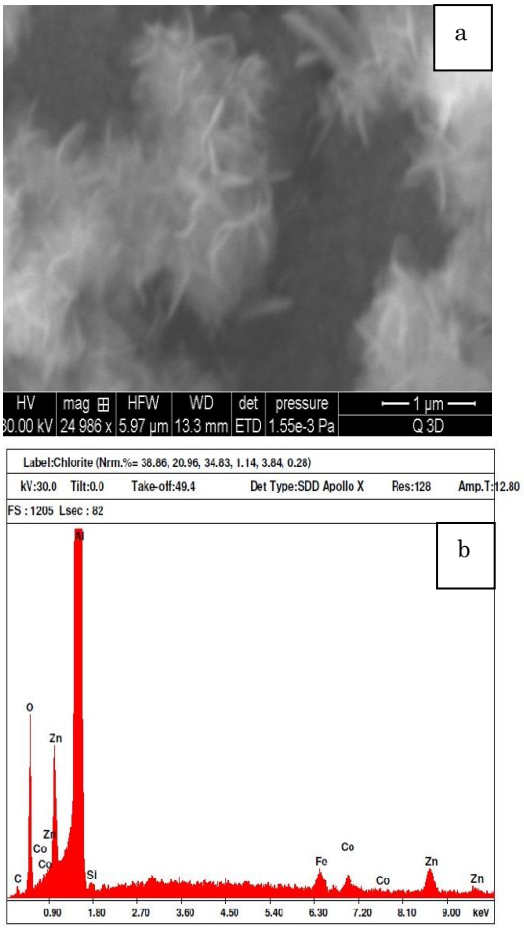

Fig. 2 – SEM image (a) and EDS spectrum (b) of $Zn_{1-x}Co_xO$ nanoparticles with content of Co $x = 0.02$

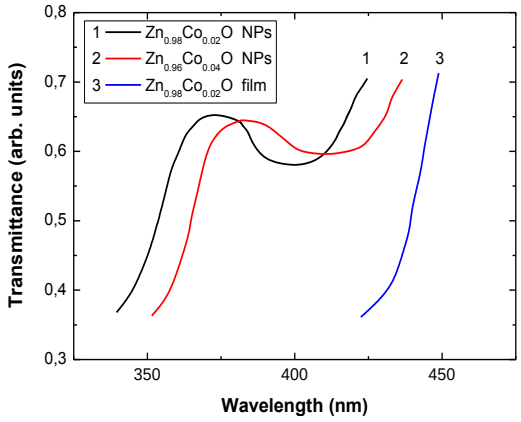

Fig. 3 – Transmittance spectra of $Zn_{1-x}Co_xO$ nanoparticles with different content of Co in spectral region near the absorption edge

absorption structure is associated with *d-d* electron transitions of Co^{2+} ions in a tetragonal crystal field. According to Hund's rule and Pauli's exclusion principle, the electronic ground state configuration has $L = 3$ and $S = 3/2$. So, the ground state spectral term is ^4F and the excited state terms are ^4P, ^2G, ^2F, ^2D and ^2P. However, when the Co^{2+} exists in the tetrahedral field, the ^4F term splits into $^4A_2(F)$, $^4T_2(F)$ and $^4T_1(F)$, with $^4A_2(F)$ being the lowest in energy and the remaining two having higher energies. The ^4P term corresponding

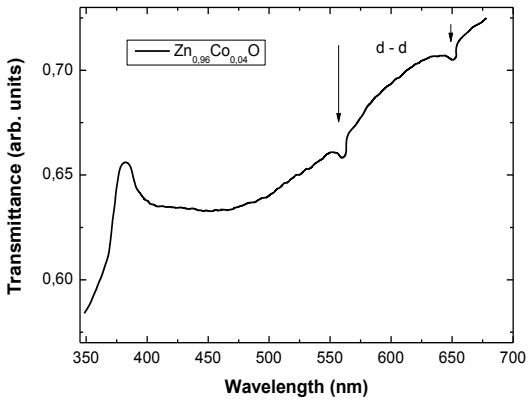

Fig. 4 – Transmittance spectrum of $Zn_{0.96}Co_{0.04}O$ nanoparticles in spectral region corresponding d-d transitions

to the first excited state does not split, but is transformed into $^4T_1(P)$. Similarly, ^2G splits into $^2A_1(G)$, $^2E(G)$, $^2T_1(G)$ and $^2T_2(G)$. In the ground state, the atom is in $^4A_2$ state. When the electron has sufficient energy, it can be excited to a higher energy state. The observed peaks were attributed to $^4A_1(F) \rightarrow {}^2A_1(G)$ and $^4A_2(F) \rightarrow {}^2E(G)$ transitions in Co^{2+} ions. The observation of these transitions in transmission spectra of our $Zn_{1-x}Co_xO$ nanostructures, thus, clearly reveals that the added cobalt atoms have been substituted by Zn^{2+}cations and are present in 2 + state. Further, an obvious red shift of the absorption edge can be observed in the Co-doped ZnO nanoparticles with increased content of magnetic impurities. This low energy shift as a function of the Co content can be explained by due to the *s*, *p-d* spin-exchange interactions between the band electrons and the localized *d*- electrons of the Co^{2+} ions [29, 30]. The exchange interaction between the transition metal ions and the band electrons give rise to a negative and a positive correction to the conduction and valence-band edges, leading to narrowing of the band gap [31].

Room temperature photoluminescence (PL) of $Zn_{1-x}Co_xO$ nanoparticles measured by exciting at 325 nm are shown in Fig. 5. The PL spectra show four peaks occurring around 390 nm, 414 nm, 503 nm and 540 nm for all samples. The first peak is in the ultraviolet (UV) region, while other three peaks correspond to violet-blue, blue and green respectively are in visible region. The UV emission band has been frequently observed in ZnO film, and can be attributed to the near band edge exciton emission because the emission energy is almost equal to the band energy of ZnO [32] estimated by UV-Vis measurements. With Co doping content increase, the UV emission center slowly shifts to long wavelength. This has been attributed to the strong exchange interactions between the d-electrons of the doping ion and the *s*- and *p*-electrons of the host band [33]. This red shift of near-band-edge emission confirms that the band gap of $Zn_{1-x}Co_xO$ decreases with increases of Co content and is in good agreement with date from optical absorption study. These shifts also are clearly reveals due to the dopant Co^{2+} ions substituted in Zn^{2+} ions. The violet-blue emission centered at around 426 nm is probably due to radiative defects related to traps existing at grain boundaries and emitted from the radiative transition between this level and the valence band [34, 35]. As Co concentration increas-

es, the peak position of blue emission shifts slightly to higher wavelength from 443 to 448 nm. The mechanism of blue emission (~ 443 nm) in ZnO low-dimensional structures is still controversial. Xu, et al. [36] synthesized single crystalline ZnO nanoplates by hydrothermal procedure and attributed the blue emission to electron transition from the level of ionized oxygen vacancies to the valence band. Gokulakrishnan et al. [37] Zr doped ZnO thin films and ascribed 443 nm centered emission band to surface defect in the ZnO films. R. Elilarassi, G. Chandrasekaran [27] and Zeng et al. [38] attributed this peak to the interstitial Zn level (Zni) and valence band. F.L. Xian, et al. [39] attributed the blue emission to the states of cobalt interstitial transition to the valence band.

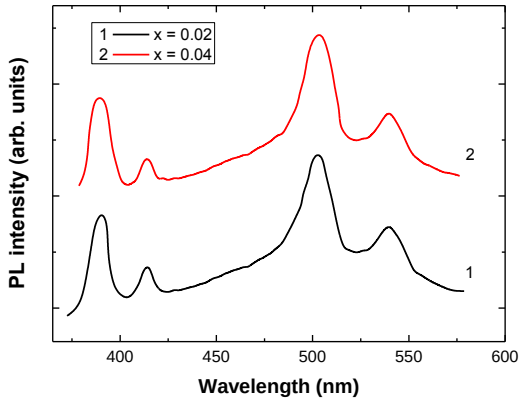

Fig. 5 – The photoluminescence spectra of $Zn_{1-x}Co_xO$ nanoparticles with different Co-content

In the latter it indicates the red shift and change in intensity of emission band with increase of Co content. The green band emission centered at ~ 538 nm is related to oxygen vacancy and it is assigned to transition from single ionized oxygen vacancy (V0) to valence band [40, 41].

4. CONCLUSIONS

In summary, $Zn_{1-x}Co_xO$ nanoparticles were successfully prepared by a pulsed laser ablation in deionized water. XRD analysis reveal that cobalt ions are successfully introduced in ZnO without changing the hexagonal wurtzite structure. The grown Co doped ZnO nanoparticles show *c*-axis preferred orientation with good crystallinity and confirms that there is no existence of a CoO or cobalt cluster peak. SEM images showed a well-defined flower-like nanoparticles. The optical absorption spectra of the nanoparticles demonstrate that the energy bang gap was found to decrease with Co content increase. Band gap narrowing effect occurs due to strong exchange interactions between d-electrons of doping ion and *s*, *p*- electrons of host lattice. The room temperature PL measurements illustrate UV emission and violet-blue, blue and green emissions in visible region. The UV emission peak originates from the radiative recombination of free excitons and their center shifts to long wavelength with increasing of Co content. Other emissions may be attributed to the radiative defects related to traps existing at grain boundaries for violet-blue emission; cobalt and zinc interstitial for blue emission; and singly ionized oxygen vacancies for green band emission, respectively.

Оптичні властивості наночастинок оксиду цинку, легованих атомами Co, одержаних методом лазерної абляції в рідині

А.Й. Савчук[1], І.Д. Столярчук[1,2], Б. Цінек[3], А. Дзедіч[3], І.В. Гадзаман[2], І.С. Вірт[2]

[1] *Чернівецький національний університет, вул. Коцюбинського, 2, 58012 Чернівці, Україна*
[2] *Дрогобицький державний педагогічний університет ім. І. Франка, вул. Стрийська, 3, 82100 Дрогобич, Україна*
[3] *Центр інновації природничих наук та інженерії, Жешувський університет, вул. Пігонія, 1, 35959 Жешув, Польща*

В роботі представлено результати експериментального дослідження спектрів поглинання та фотолюмінесценції наночастинок ZnCoO, отриманих методом імпульсної лазерної абляції твердотільних мішеней у рідкому середовищі. Структурні дослідження проводились із використанням рентгенівської дифракції та скануючої електронної мікроскопії (СЕМ). Отримані дані свідчать про ріст нанокристалів в гексагональній вюрцитній структурі з переважною орієнтацією (002) без утворення вторинних фаз. Результати СЕМ демонструють отримання складних, квітко-подібних утворень наночастинок ZnCoO. В спектрах поглинання колоїдних наночастинок виявлено короткохвильовий зсув краю фундаментального поглинання, зумовлений квантово-розмірним ефектом. Зростання концентрації кобальту приводить до довгохвильового зсуву краю фундаментального поглинання, що зумовлено проявом *s*, *p* - *d* обмінної взаємодії зонних носіїв із локалізованими спінами магнітної компоненти. В спектрах фотолюмінесценції, виміряних при кімнатній температурі, спостерігаються чотири смуги випромінювання, зумовлені екситонними переходами на краю фундаментального поглинання та наявними домішками і дефектами.

Ключові слова: $Zn_{1-x}Co_xO$, Наночастинка, Нанокристал, Імпульсна лазерна абляція в рідині, Х-променева дифракція, Поглинання, Фотолюмінесценція.

Оптические свойства наночастиц оксида цинка, легированных атомами Co, полученных методом лазерной абляции в жидкости

А.Й. Савчук[1], И.Д. Столярчук[1,2], Б. Цинэк[3], А. Дзедич[3], И.В. Гадзаман[2], И.С. Вирт[2]

[1] *Черновицкий государственный университет, ул. Коцюбинского, 2, 58012 Черновцы, Украина*
[2] *Дрогобыжский государственный педагогический университет им. И. Франко, ул. Стрийска, 3, 82100 Дрогобыч, Украина*
[3] *Центр инновации природнических наук и инженерии, Жешувский университет, ул. Пигония, 1, 35959 Жешув, Польша*

В работе представлены результаты экспериментального исследования спектров поглощения и фотолюминесценции наночастиц ZnCoO, полученных методом импульсной лазерной абляции твердотельных мишеней в жидкой среде. Структурные исследования проводились с использованием рентгеновской дифракции и сканирующей электронной микроскопии (СЭМ). Полученные данные свидетельствуют о росте нанокристаллов в гексагональной вюрцитной структуре с преимущественной ориентацией (002) без образования вторичных фаз. Результаты СЭМ демонстрируют получения сложных, цветок-подобных образований наночастиц ZnCoO. В спектрах поглощения коллоидных наночастиц обнаружено коротковолновый сдвиг края фундаментального поглощения, обусловленный квантово-размерным эффектом. Рост концентрации кобальта приводит к длинноволновому сдвигу края фундаментального поглощения, обусловленного проявлением *s*, *p*- *d* обменного взаимодействия зонных носителей с локализованными спинами магнитной компоненты. В спектрах фотолюминесценции, измеренных при комнатной температуре, наблюдаются четыре полосы излучения, обусловленные экситонными переходами на краю фундаментального поглощения и имеющимися примесями и дефектами.

Ключевые слова: $Zn_{1-x}Co_xO$, Наночастицы, Нанокристаллы, Импульсная лазерная абляция в жидкости, Х-лучевая дифракция, Поглощение, Фотолюминесценция.

REFERENCES

1. A. Dogan, S. Avrutin, V. Cho S. J., H. Morkoc, *J. Appl. Phys.* **98**, 041301 (2005).
2. D.D. Awschalom, D. Loss, N. Samarth, *Semiconductor Spintronics and Quantum Computation* (Springer: Berlin: 2002).
3. S.J. Pearton, W.H. Heo, M. Ivill, D.P. Norton, T. Steiner, *Semocond. Sci. Technol.* **19**, R59 (2004).
4. S.J. Pearton, D.P. Norton, K. Ip, Y.W. Heo, T. Steiner, *Prog. Mater.Sci.* **50**, 293 (2005).
5. K.C. Barick, M. Aslam, V.P. Deavid, D. Bahadur, *J. Phys. Chem. C* **112**, 15163 (2008).
6. O.D. Jayakumar, C. Sudakar, A. Vinu, A. Asihana, A.K. Tyagi, *J. Phys. Chem. C* **113**, 4814 (2009).
7. I. Djerdj, G. Garnweitner, D. Arcon, M. Pregeli, Z. Jaqlicic, M. Niedegrberger, *J. Mater. Chem.* **18**, 5208 (2008).
8. L. Zhang, X. Liu, C. Geng, H. Fang, Z. Lian, X. Wang, D. Shen, Q. Yan, *Inorg. Chem.* **52**, 10167 (2013).
9. W. Hao, J. Li, H. Xu, J. Wang, T. Wang, *ACS Appl. Mater. Interf.* **2** No 7, 2053 (2010).
10. S. Zhang, F. Hu, J. He, W. Cheng, Q. Liu, Y. Jiang, Z. Pan, W. Yan, Z. Sun, S. Wei, *J. Phys. Chem. C* **117**, 24913 (2013).
11. A.I. Savchuk, V.I. Fediv, S.A. Savchuk, A. Perrone, *Superlattice. Microstructur.* **38** No 4, 421 (2005).
12. A.I. Savchuk, V.P. Makhniy, V.I. Fediv, G.I. Kleto, S.A. Savchuk, *phys. status solidi a* **206** No 9, 2177 (2009).
13. A.I. Savchuk, V.P. Makhniy, V.I. Fediv, G.I. Kleto, S.A. Savchuk, A. Perrone, L. Cultrera, *IOP Conf. Series: Mater. Sci. Eng.* **8** No 1, 012042 (2010).
14. N.G. Semaltianos, S. Logothetidis, W. Perrie, S. Romani, R.J. Potter, M. Sharp, K.G. Watkins, *Appl. Phys. Lett.* **95** No 3, 033302 (2009).
15. H. Usui, Y. Shimizu, T. Sasaki, N. Koshizaki, *J. Phys. Chem. B* **109** No 1, 120 (2005).
16. R.K. Thareja, S. Shukla, *Appl. Surf. Sci.* **253** No 22, 8889 (2007).
17. S.C. Singh, R. Gopal, *Physica E* **40** No 4, 724 (2008).
18. S.C. Singh, R. Gopal, *Appl. Surf. Sci.* **258** No 7, 2211 (2012).
19. M.A. Gondal, Q.A. Drmosh, Z.H. Yamani, T.A. Saleh, *Appl. Surf. Sci.* **256** No 1, 298 (2009).
20. G. Compagnini, M. Sinatra, G.C. Messina, G. Patanè, S. Scalese, O. Puglisi, *Appl. Surf. Sci.* **258** No 15, 5672 (2012).
21. A.I. Savchuk, A. Perrone, A. Lorusso, I.D. Stolyarchuk, O.A. Savchuk, O.A. Shporta, *Appl. Surf. Sci.* **302**, 205 (2014).
22. A. Zocco, A. Perrone, A. Luches, R. Rella, A. Klini, I. Zergiot, C. Fotakis, *Thin Solid Films* **349** No 1, 100 (1999).
23. P.K. Samanta, S.K. Patra, P.R. Chaudhuri, *Physica E* **41** No 4, 664 (2009).
24. S. Chakraborty, A.K. Kole, P. Kumbhakar, *Mater. Lett.* **67** No 1, 362 (2012).
25. P. Ramasamy, J. Kim, *Mater. Lett.* **93**, 52 (2013).
26. J.H. Kim, H. Kim, D. Kim, S.G. Yoon, W.K. Choo, *Solid State. Commun.* **131**, 677 (2004).
27. K.J. Kim, Y.R. Park, *Appl. Phys. Lett.* **81** No 8, 1420 (2002).
28. L. Wei, Z. Li, W.F. Zhang, *Appl. Surf. Sci.* **255**, 4992 (2009).
29. X. Xu, C. Cao, *J. Alloy Compd.* **501**, 265 (2010).
30. J.K. Furdyna, *J. Appl. Phys.* **64** No 4, R29 (1988).
31. Y.G. Wang, S.P. Lau, H. Lee, S.F. Yu, B.K. Tay, X.H. Zhang, H.H. Hng *J Appl. Phys.* **94**, 354 (2003).
32. B. Panigrahy, M. Aslam, D. Bahadur, *J. Phys. Chem. C* **114**, 11758 (2010).
33. S. Kumar, S. Basu, B. Rana, A. Barman, S. Chatterjee, S.N. Jha, A.K. Ghosh, *J. Mater. Chem. C* **2** No 3, 481 (2014).
34. L.J. Zhuge, X.M. Wu, Z.F. Wu, X.M. Yang, X.M. Chen, Q. Chen, *Mat. Chem. Phys.* **120**, 480 (2010).
35. F. Xu, Z.Y. Yuan, G.H. Du, M. Halasa, B.L. Su, *Appl. Phys. A* **86** No 2, 181 (2007).
36. V. Gokulakrishnan, S. Parthiban, K. Jeganathan, K. Ramamurth, *Appl. Surf. Sci.* **257** No 21, 9068 (2011).
37. R. Elilarassi, G. Chandrasekaran, *J. Mater. Sci.: Mater. Electron.* **24**, 96 (2013).
38. H. Zeng, G. Duan, Y. Li, S. Yang, X. Xu, W. Cai, *Adv. Funct. Mater.* **20** No 4, 561 (2010).
39. F.L. Xian, L.H. Xu, X.X. Wang, X.Y. Li, *Cryst. Res. Technol.* **47** No 4, 423 (2012).
40. S. Chakraborty, P. Kumbhakar, *Indian J. Phys.* **88** No 3, 251 (2014).
41. J. Ding, X. Yana, Q. Xue, *Mater. Chem. Phys.* **133**, 405 (2012).